ELSEVIER

Marine Geology 187 (2002) 329–345

MARINE GEOLOGY
INTERNATIONAL JOURNAL OF MARINE GEOLOGY, GEOCHEMISTRY AND GEOPHYSICS

www.elsevier.com/locate/margeo

Interaction between breaking/broken waves and infragravity-scale phenomena to control sediment suspension transport in the surf zone

G.G. Smith *, G.P. Mocke

CSIR, Division of Water, Environment and Forestry Technology, Jan Cilliers Street, 7599 Stellenbosch, South Africa

Received 30 March 2001; accepted 23 May 2002

Abstract

Time series of near-bed sediment, water-level and velocity were measured in the field and laboratory and analysed to investigate (a) the role of breaking/broken waves, (b) the predominance of infragravity-scale transport processes in the surf zone, and (c) the influence of infragravity processes in creating the right conditions for suspension by breaking/broken waves. Instantaneous suspended sediment concentrations were measured using optical backscatter sensors, which were found to be sensitive to sediment size, cohesive sediment in suspension and bubbles. A simple numerical filter was applied to remove the erroneous bubble signal. Suspension was found to be correlated with wave breaker bores and an associated increase in high-frequency velocities, the latter deemed to be caused by surface-generated turbulence. Infragravity-scale sediment transport flux was found to be more significant than incident-scale flux in the transition and inner surf zones. Sediment suspension was further found to be related to the onset of lower water-levels associated with infragravity wave action, which corresponded with a predominance of breaking/broken waves. These breaking/broken waves (which are induced by the low water-level) are deemed to be the cause of this suspension.

Keywords: wave breaker turbulence; surf zone; nearshore processes; sediment suspension; optical backscatter sensor; sediment transport

1. Introduction

An improved understanding of the processes of suspension and transport of sediment in the surf zone is essential in order to predict sediment transport (and therefore morphology) accurately and thus to solve coastal engineering problems in this highly dynamic region. Measurements in the surf zone have highlighted the occurrence of elevated levels of sediment concentration over the entire water depth, unlike the case in non-breaking waves where sediment is generally confined to a thin layer near the bed (Shibayama and Winyu, 1993). Observations have further highlighted the strong influence of breaker type and surf zone position on suspended sediment response (Kana, 1978; Yu et al., 1993). Apart from these breaking and broken wave related influences, surf zone

* Corresponding author.
E-mail address: gsmith@csir.co.za (G.G. Smith).

0025-3227/02/$ – see front matter
PII: S0025-3227(02)00385-7

sediment transport processes are distinguishable from those of the shoaling region by the occurrence of more extreme oscillatory wave motions (particularly on an infragravity time scale) and time-averaged flows.

Upon the initiation of wave breaking, wave orbital motions dominate the velocity structure and wave shape. But as the wave breaking process progresses, orbital velocities are reduced and vortex motions and associated turbulence dominate the wave velocity field (Yu et al., 1993). In assessing the influence of wave breaking on the sediment suspension process, Nielsen (1984) and Shibayama et al. (1986) have identified the action of the large-scale vortices generated coincident with wave plunging. The vortex and associated turbulence are responsible for significant sediment suspension, with field measurements of Kana (1978) showing concentrations under plunging waves of up to an order of magnitude greater than equivalently sized spilling and non-broken waves. However, the essentially two-dimensional vortices are restricted to the transition zone (i.e. the region defined as extending from the commencement of wave breaking to a point where bores are fully developed), shorewards of which the surf zone is characterised by a surface bore or roller, in the so-called inner zone.

Experimental measurements through the inner 'roller' region (Stive, 1980; Nadaoka and Kondoh, 1982) have revealed the presence of a turbulence-generating layer in the vicinity of the surface roller from which turbulence is transported downwards. Nadaoka et al. (1989) have furthermore identified an eddy structure whereby the surface roller is dominated by a nearly two-dimensional flow structure, bounded below by strongly three-dimensional obliquely descending eddies bringing highly intermittent turbulence to the bottom. The dominant action of this turbulence for sediment suspension is verified by means of concentration measurements and visualisation studies made by Sato et al. (1990) and Nadaoka et al. (1988) in a wave flume. Computations using turbulent closure models with a turbulence source in the surface roller have been shown by Deigaard et al. (1986) and Mocke and Smith (1992) to result in favourable predictions of the turbulent flow structure and suspended sediment concentrations measured through the water column under breaking waves.

For the most part, past studies of surf zone sediment suspension have highlighted the role of infragravity-scale waves and currents (e.g. Aagaard and Greenwood, 1994; Beach and Sternberg, 1988) without recognising the role of wave breaker- and bore-induced vortices and turbulence (e.g. as described in Yu et al., 1993). From an analysis of data at both a barred beach and a non-barred beach Greenwood et al. (1991) found an increase in sediment transport flux at low frequencies in the surf zone (relative to the shoaling region). Aagaard and Greenwood (1994) maintained that infragravity waves contribute significantly to the entrainment as well as the transport of sediment, by enhancing near-bed velocities. These authors noted that although incident-scale processes play a significant role in the shoaling region, whereby sediment suspension is both induced by and phase-linked to orbital velocities, they tend to play a secondary role relative to infragravity-scale and time-mean processes and flows in the surf zone. Barkaszi and Dally (1992) further found that the oscillatory structure of sediment suspension occurring offshore is lost in the region of initial wave breaking, where they found that peaks in concentration occur randomly, even for regular waves. However, in some cases incident-scale processes in the surf zone are found to be relevant, with Greenwood et al. (1991) finding that incident-scale onshore transport was more prominent than that occurring offshore, on a non-barred nearshore profile. This is reported to be due to an increase in velocity skewness under the non-linear breaking waves.

The notion that infragravity motions are responsible for sediment entrainment originated from the observation that suspension coincided with infragravity-scale phenomena, for example low water-levels and/or seaward flow. It was assumed that the mechanism for the suspension was the infragravity flow per se. However, it has been found that the increase in suspension at infragravity scales is higher than would be expected from a bed shear stress scaling on the instantaneous horizontal velocity (Hanes, 1991). This discrepancy could be explained by a lack of recognition of

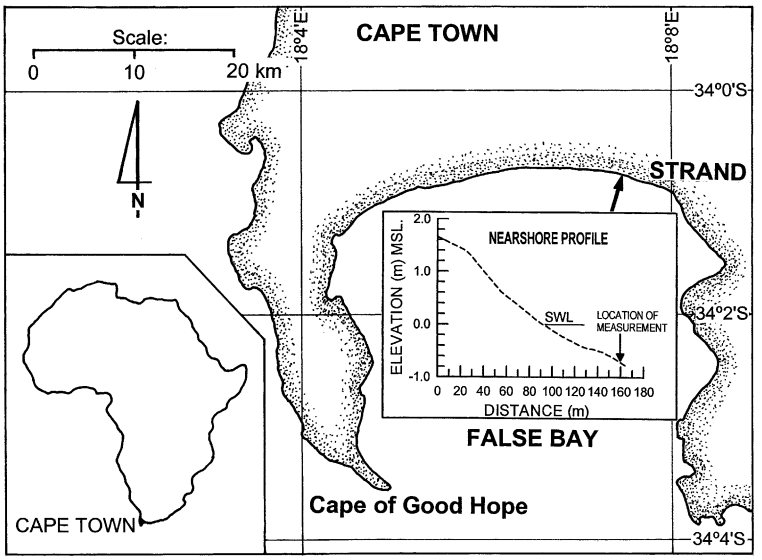

Fig. 1. Strand measurement site location and profile cross-section.

wave breaking processes, which interact with infragravity motions. Possible examples of the interaction of wave breaking and infragravity sediment suspension and transport phenomena are (1) more energetic wave breaking is likely to occur in the shallower trough of long waves, and (2) surface-generated turbulence/eddies have less distance to travel to reach and stir the sediment bed in shallower water associated with long-wave troughs. In addition, (3) a simple phase-linking between long waves and groups of higher waves/bores can occur. The latter has been found to be associated with a progressive stirring effect (Smith et al., 1995; Villard et al., 1999) whereby suspension events are related to antecedent wave conditions.

The primary objective of the present study is to investigate and quantify the role of wave breaking flow fields in the suspension and transport of sediments in the surf zone. Although breaking is confined to incident waves, the investigation does not ignore the important influence of infragravity-scale processes. Attention is however focused on the manner in which long-wave phenomena serve to enhance the influence of wave breaking. A secondary objective of the study is to assess the integrity of optical backscatter sensor (OBS) measurements, particularly in response to breaker-entrained bubbles.

2. Measurement exercises

2.1. Strand field site

A one-day field exercise was conducted at Strand, situated in the south-facing False Bay (Fig. 1). The spring and neap tidal ranges in this region are around 1.5 and 0.6 m respectively. The site is significantly sheltered from dominant waves approaching from the westerly and easterly sectors, while an offshore reef also plays a major role in sheltering the region. As a result, waves at the site generally range from about 0.5 to 2 m, with dissipative conditions reflected in the fine sediment ($d_{50} = 154$ μm) and mildly sloping (1:40) beach (Fig. 1).

Instrumentation was attached to a light scaffold frame resembling that of Black and Rosenberg (1991). Two electromagnetic current meters, constructed at the CSIR, were deployed to measure currents at 0.28 and 0.71 m from the bed. Each current meter incorporated a pressure sensor (respectively at 0.913 and 1.343 m from the bed). Three OBS for measuring sediment concentration were deployed at variable elevations ($z = 0.09$–0.34 m) that corresponded with three suction samplers. A wave gauge (NSRFC, 1975) was also deployed. The frame was manually deployed, jetted into the

sandy bed with compressed air and secured with a stay at each corner. The OBS measurements were transmitted by means of a cable to the shore station established in a vehicle on the beach. All other measurements were logged in situ.

Under relatively calm conditions with winds generally under five knots, wave breaking ranged from spilling to mildly plunging. Significant wave heights over the duration of the exercise averaged 0.98 m while the average wave period was 13.3 s. The water depth at the frame decreased with the ebb tide from about 1.8 m to about 1.1 m during the exercise. As a result, at the start of the exercise the frame was situated in a region of occasional breaking, while later on the frame was situated well within the inner surf zone. Data return from the instruments ranged from 94% to 100%, for a measurement period of five hours (CSIR, 2000).

2.2. The Delta Flume 1993 experiment (LIP11D)

The LIP11D experiment, carried out during April–June 1993 in the Delta Flume at the De Voorst laboratory of Delft Hydraulics in the Netherlands, was a large-scale wave-flume test supported by the 'Large Installations Plan' (LIP) of the European Union MAST programme. The main objective of the experiment was to generate hydrodynamic and morphodynamic data on a natural 2DV beach under equilibrium, erosive and accretive conditions. The authors participated in this exercise and provided three OBS's for measuring instantaneous suspended sediment concentration.

Fig. 2 is a schematic presentation of the Delta Flume showing LIP11D instrumentation. For further details of instrumentation, flume geometry, water-levels, wave conditions tested, etc. reference is made to Sanchez-Arcilla et al. (1994). For the purpose of the present study, use was primarily made of instrumentation attached to a roving carriage deployed at various locations across the profile in the 220-m-long flume (Fig. 2). Relevant instrumentation affixed to the carriage included:

- five OBS (at elevations above the bed of 0.05 (two sensors), 0.10, 0.13, and 0.15 m);
- a sediment concentration sampler (operated with a peristaltic pump) with 10 suction tubes (at elevations above the bed of 0.05, 0.075, 0.10, 0.18, 0.255, 0.40, 0.65, 1.05, and 1.55 m);
- a series of electromagnetic flow meters (at elevations above the bed of 0.10, 0.20, 0.40, 0.70, and 1.10 m); and
- an overhead video camera.

The instruments were aligned with approaching wave fronts. The carriage was moved every hour during each test, so that an extensive set of mea-

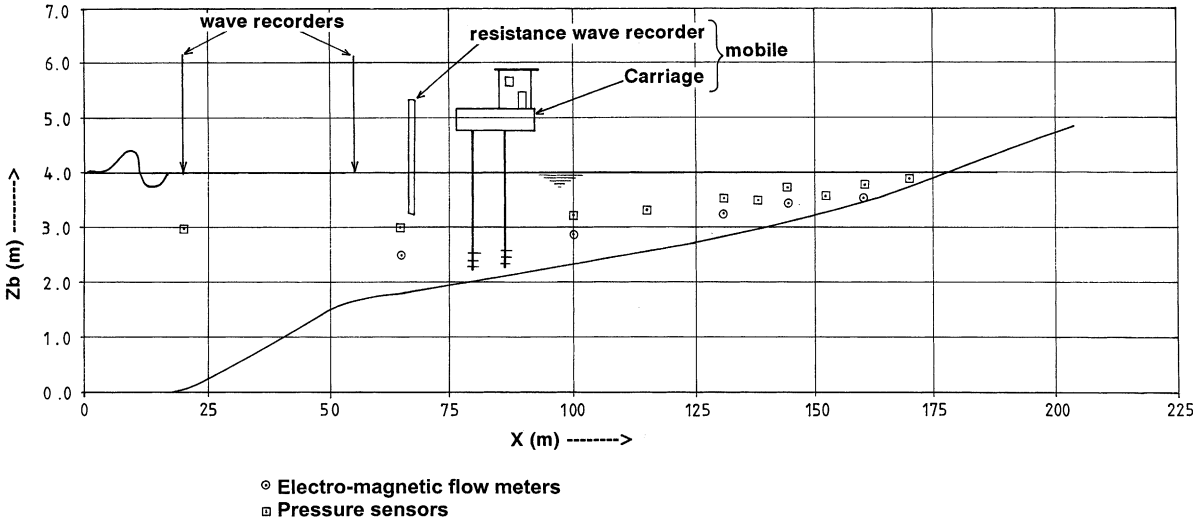

Fig. 2. Schematic of the Delta Flume showing LIP11D instrumentation deployed at 10 measurement stations.

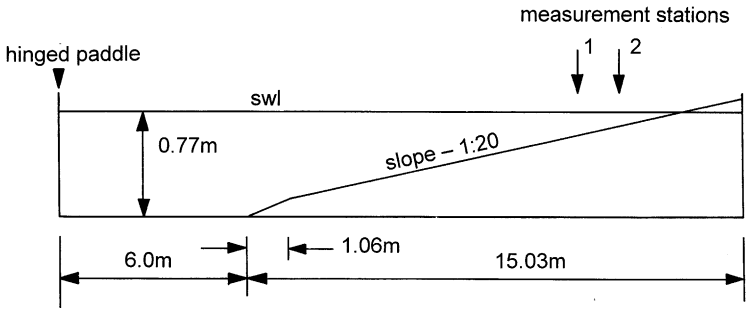

Fig. 3. CSIR wave-flume dimensions and measurement stations.

surements was obtained at several sites across the beach profile. In addition, an automatic depth sounding system (PROVO) was used periodically from the carriage to measure beach profiles (Sanchez-Arcilla et al., 1994).

The present study makes use of measurements taken during the second series of tests at LIP11D (Tests 2A and 2B). Test 2A was commenced with a Dean-type beach profile, with a dune included, while Test 2B commenced with the profile remaining from Test 2A. Narrow-banded random waves were generated. The significant wave height at the wave generator was 0.9 m for Test 2A and 1.4 m for Test 2B. The wave period of peak energy for both tests was 5 s, with a water-level of 4.1 m.

Each test was divided into a number of hours (total 12 h), during each of which continuous measurements of flows, pressures, water elevations and instantaneous sediment concentrations were made at a sampling frequency of 10 Hz. Each signal was low-pass filtered by an analogue filter at 5 Hz before storage.

2.3. CSIR wave-flume experiment

A set of measurements was obtained in a small wave flume with a partially sedimentary bed. The wave flume (Fig. 3) was 21 m long, 0.745 m wide and 1.0 m deep. A fixed-bed slope of 1:20 was built into the flume. A sand pan was fitted on the flume bed in the surf zone, 3 m from the still water line. The pan was 1.20 m long, 0.745 m wide and 30 mm deep. Wave measurements were taken with two wave gauges, one situated 5.77 m from the wave generator and the other fixed at the same location as the OBS, on a moveable carriage.

Two regular wave test conditions were applied for all measurements:

- plunging waves of 0.11 m height, and a period of 2.5 s;
- spilling waves of 0.17 m height and a period of 1.2 s.

Under each wave condition five sets of measurements were taken, at various elevations varying from 30 to 90 mm above the bed, near the position of wave breaking and in the well-developed surf zone. Time series of the concentrations and wave heights were recorded at a frequency of 10 Hz, with bursts lasting 204.8 s. An additional test was conducted by measuring at the plunge point without sediment, the object being to investigate the role of bubbles in causing erroneous sediment concentration measurements.

3. Analysis methods

A low-pass digital filter, as described by Kaiser and Reed (1977), was employed both for filtering out undesirable signal noise and for resolving low-frequency data, such as water-level fluctuations on an infragravity scale. In addition, the filter was used to isolate high-frequency data, such as resolving high-frequency events in the velocity record.

Cross-correlation was employed to assess relationships between two time series (e.g. sediment concentration and flow velocity). The IMSL routine CCF (IMSL, 1991) was used for this purpose.

Although there are inherent limitations to applying spectral analysis to the 'spiky' non-linear time series of sediment concentration, this method has been extensively used, with due attention given to confidence limits, in order to investigate periodicity in the time series (e.g. Beach and Sternberg, 1988; Greenwood et al., 1991; Hanes, 1991). The IMSL spectral analysis routine DSSWD was employed (IMSL, 1991), using a Parzen smoothing window. Care was taken in ensuring that the record length and spectral parameters were such that sufficient resolution bandwidth and confidence in spectral estimates were obtained, i.e. such that all the peaks resolved and referred to in this study were statistically significant. A Nyquist/cut-off frequency of 2.0 Hz was employed for the Strand data, while in the case of the LIP data, a cut-off frequency of 2.5 Hz was employed.

The IMSL routine CSSWD was used for the calculation of the cospectrum, used for estimating the components of sediment transport flux as a result of oscillatory wave motion, as described in Huntley and Hanes (1987). The same cut-off frequencies were used as those for the one-dimensional spectra.

The smoothed instantaneous wave energy history (SIWEH) function was used to compute the distribution of energy of vertical velocity along the time axis. The SIWEH function (Funke and Mansard, 1979) is defined as follows:

$$E(T) = \frac{1}{T}\int_{-T/2}^{T/2} w^2(t+\tau)\mathrm{d}\tau \quad (1)$$

where $w(t)$ is the time series of vertical velocity and T is the time period over which the function is applied.

The Bartlett smoothing window was used in tandem with the SIWEH function, which was used to isolate events of high-frequency oscillatory motion in the flow, manifested by a positive peak coincident with these events, in the time series of flow.

Sediment flux calculations were made. The local net sediment transport flux is determined by:

$$uc_{\mathrm{net}} = 1/n \sum uc \quad (2)$$

where n is the sample size, u the instantaneous horizontal velocity and c the instantaneous sediment concentration.

The local sediment transport flux due to the time-mean components of the flow (e.g. undertow and time-mean sediment concentration) is defined by:

$$uc_{\mathrm{mean}} = 1/n \sum c \cdot 1/n \sum u \quad (3)$$

The local sediment transport flux due only to oscillatory wave motion is defined by:

$$uc_{\mathrm{osc}} = uc_{\mathrm{net}} - uc_{\mathrm{mean}} \quad (4)$$

4. Sediment concentration data pre-processing

4.1. OBS calibration

The method used to calibrate the OBS involved stirring and therefore suspending sediment in a nine-litre bucket of water by means of a pair of rotating propellers (similar to Black and Rosenberg, 1991). The method was used because of its simplicity. Increasing concentrations of sediment were added to the bucket and each time the average voltage signal corresponding to that concentration was recorded. An expected linear relationship (Black and Rosenberg, 1994; Kineke and Sternberg, 1992) between OBS voltage signal and concentration was obtained ($R^2 = 0.993$).

4.2. Signal treatment

The authors have found that a reliable calibration alone is not always adequate to obtain reliable OBS concentration measurements. Sources of error that must be considered include: sand particle size effects, fine (cohesive) sediment effects, organic material in suspension, and bubbles.

4.2.1. Sand size effects

The size distribution of suspended sediment as compared to sediment sampled from the bed at the same location is generally different. As the OBS is known to be sensitive to grain size (Conner and De Visser, 1992), calibration based on

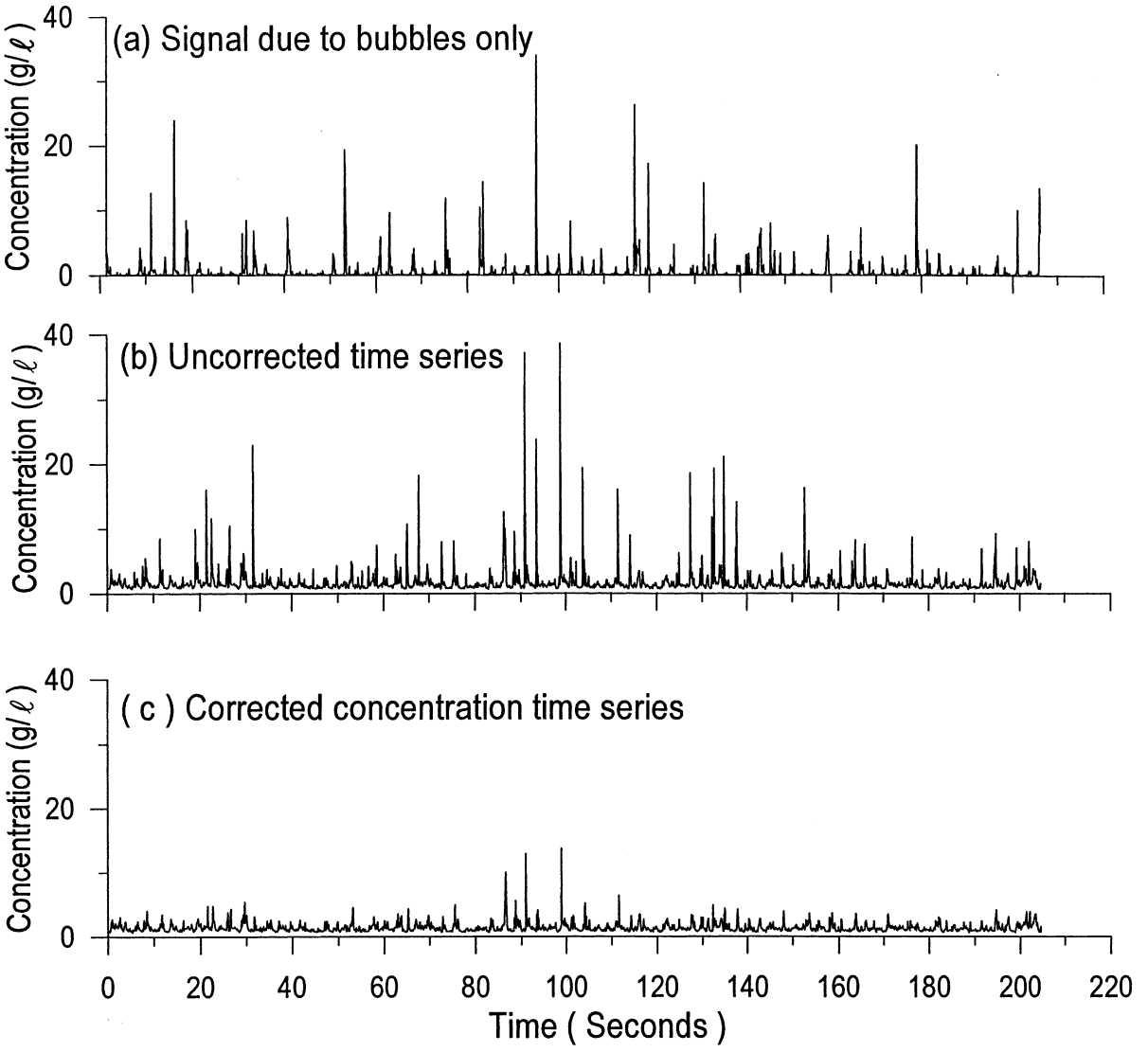

Fig. 4. Bubbles and sediment concentration time series measured to investigate the effect of aeration at breaking on OBS measurements, in the CSIR wave flume (plunging waves, $z = 0.09$ m, $h = 0.17$ m).

sediment sampled from the bed (rather than the suspended sediment) could result in erroneous concentrations. Based on the work of Black and Rosenberg (1994), a maximum error of only 5% due to sand size effects was estimated, for the particular range of sediment sizes for the present study. Ludwig and Hanes (1990) similarly found that the suspended sediment sand size does not greatly affect sediment sensor gain.

The extreme case of OBS sensitivity to sediment size is for cohesive sediments, for which the OBS is an order of magnitude more sensitive than for beach sands. This is particularly problematic if the concentration of cohesive sediment varies, making it difficult to distinguish between the portion of the OBS signal due to suspended sand and the portion due to suspended fines (Ludwig and Hanes, 1990). By recording a sand/mud mixture at exactly the same location with two OBS of differing sensitivities, a technique of separating

the recordings of the two sediment sizes can be employed (Green and Boon, 1993), while Battisto et al. (1999) employ an alternative method of cutting off the continuous 'background' OBS signal which is determined to be due to fines. In a similar attempt to record and remove the portion of the signal due to fine material in suspension, measurement was continued for several minutes after wave generation ceased in the LIP11D experiment. This approach was only partially successful because fluctuations of the 'background' concentration occurred during measurement. This was resolved by correcting concentrations using time-averaged sediment concentrations obtained by means of pumping.

4.2.2. Particulate organic matter

Isolated spikes in the OBS signal record were observed in the LIP11D data. It is thought that these are caused by particles of organic matter (peat), which were observed in the Delta Flume. Such spikes were removed when identified on only one of the OBS records (if a spike is evident on all three OBS records it was assumed to be caused by a suspension event and was not removed), as applied by Barkaszi and Dally (1992). In addition, where applicable, concentration time series were low-pass filtered with a Kaiser filter (Kaiser and Reed, 1977) in order to remove noise that occurred at a frequency above 1 Hz.

4.2.3. Bubbles

The occurrence of bubbles, particularly in the surf zone, can cause erroneous measurement of sediment concentration with the OBS. Tests involving the release of air bubbles opposite the OBS indicated that an error of a few percent could occur in the concentration time series when air is significantly entrained during wave breaking and/or bore progression. Similarly, Black and Rosenberg (1994) found the OBS signal due to air entrainment during calibration to be 5–10% greater than the still water value. Observing that the volume of air entrained during calibration was visually much greater than that expected under broken waves, they concluded that the effect on the OBS of air entrainment in the field should be small.

The effect of bubbles on OBS measurements made in the small CSIR wave flume was further investigated. Fig. 4b illustrates concentration time series measurements of sediment suspended from a tray on the bed of the flume at the breaking region with plunging waves. Severe spikes are observed in the data, which were found to coincide with peaks in the water elevation record, i.e. they coincide with the plunging waves. Considering the nature of both sediment suspension and subsequent settling velocities (of the order of 25–70 mm/s for the sand used) the events were considered too rapid to be caused by suspended sediment. Rather, the intermittent and spiky nature of these events (generally lasting about 0.1 s) is characteristic of the occurrence of air bubbles (the observed bubbles which are about 5 mm in diameter ascend at an estimated 300 mm/s).

The approximation of the erroneous OBS 'concentration' signal that occurred only due to aeration was investigated by running the experiment with exactly the same conditions but without sediment in the flume. The result is shown in Fig. 4a. While the time average of the former concentration time series is 1.68 g/l, the latter is 0.55 g/l. Ignoring non-linear interactions between bubbles and sand grains, this indicates that bubbles contribute to an average error of 33% of the concentration signal over this data record.

An attempt was made to eliminate the spikes caused by bubbles by employing a simple numerical routine similar to that of Sato et al. (1990). Each concentration value was evaluated relative to the previous three in the time series. Three data points represent 0.3 s; it was found that contamination by another bubble event (generally lasting 0.1 s) in this period was unlikely, but the period is long enough to determine the short-term trend for the evaluation of a concentration correction. If a concentration value was found to be significantly higher than the previous three (by a margin of 0.7 g/l in this instance, as defined by the user from observation of the time series), then the average of the previous three values replaced it. The result of applying this criterion to the uncorrected time series is shown in Fig. 4c, where the signal error due to air bubbles was reduced by an average of 52%.

5. Results

5.1. The role of breaking and broken waves

5.1.1. Transition zone

In investigating sediment suspension in response to incident waves, the occurrence of suspension events (i.e. distinct increases in concentration relative to the quasi-steady background concentration occurring between events) relative to the wave phase was investigated for the LIP transition zone data (53-min record). In this analysis, an event was defined as any sediment concentration above twice the average background concentration. The phase of each individual record of the time series that occurs within an event was determined, relative to the wave crest, and categorised to form a histogram (Fig. 5). As can be seen, sediment suspension in the form of events tends to occur more frequently during the first half of the wave phase after the peak, tapering off before the following wave peak occurs. This phenomenon is probably due to the influence of wave breaking, particularly for plunging waves, which cause high vortex action soon after the wave peak.

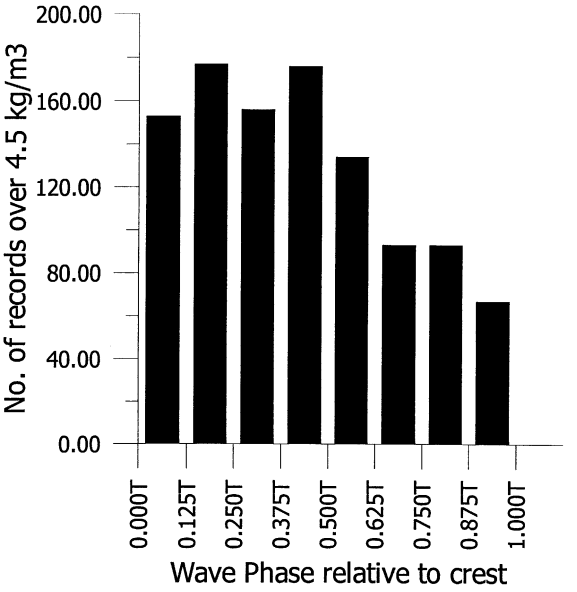

Fig. 5. Histogram illustrating the phase (relative to the wave peak) of the occurrence of sediment suspension concentrations that are significantly higher than the relatively constant background level (i.e. above 4.5 kg/m^3). LIP Test 2A, $X = 138$ m.

With the use of video recordings, the distinction between broken/breaking and unbroken waves could be made. It was observed that, despite some of the unbroken waves being higher, suspension tended to occur after the occurrence of a series of breaking/broken waves (Fig. 6).

The percentage of broken waves or bores (as opposed to unbroken waves) occurring just before each sediment suspension event (for a 53-min period of LIP Test 2A0506) was determined. For the sake of simplicity, plunging waves (comprising only 4% of the waves in this analysis) are included with developed bores. Considering only the waves occurring immediately before events, 66% of these were bores. Considering two waves prior to suspension events, 58% of these were found to be bores, while the percentage of bores three waves before events was 51%. These percentage occurrences are greater than the average percentage of bore occurrence during the measurement hour (i.e. 38%), indicating that turbulence (and convection/vortex motions) as induced by bores (and breaking waves) plays a significant role in sediment suspension. Furthermore, the significance of high bore occurrence up to three waves prior to events supports the idea of progressive stirring by successive waves that then induce suspension.

High-frequency 'events' (or concentrations of oscillatory activity) in the vertical velocity were seen to occur simultaneously with/or just after the occurrence of bores. These events are evident in the high-frequency velocity record of Fig. 6 from LIP Test 2A0506 (obtained by high-pass filtering of the vertical velocity with a cut-off frequency of 1 Hz). Although these events are not strictly within the recognised frequency range for turbulence (the measurement frequency being 5 Hz), they seem to be indicative of turbulent motion generated by bores. This concept is supported by Hattori and Aono (1985), who found that a large portion of turbulent energy is transferred from large-scale eddies to frequencies between 1 and 10 Hz upon breaking. On closer observation it may be noted that the high-frequency, small-amplitude velocity signals also occur in the

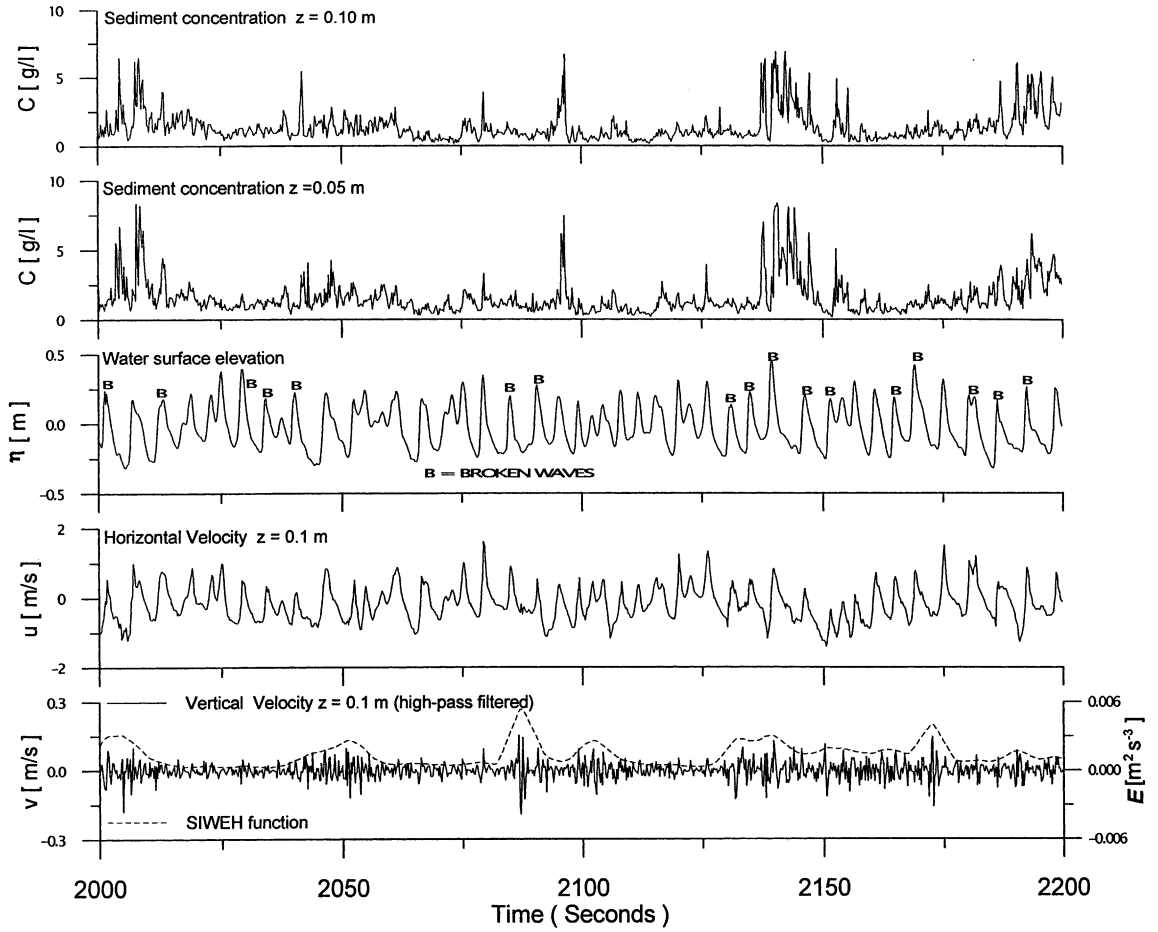

Fig. 6. Time series of sediment concentration and colocated velocities and surface elevations measured a few metres shoreward of the peak of the breaker bar for LIP Test 2A ($X = 138$ m), and (bottom) the SIWEH function applied to the high-frequency (> 1 Hz) vertical velocity record.

horizontal velocity record, which indicates that they are three-dimensional. This may be a manifestation of three-dimensional eddies, as proposed by Nadaoka et al. (1988).

Further investigation of eddies made use of the SIWEH function (Eq. 1), by means of which the energy of these events in the high-frequency vertical velocity time series is identified and represented (Fig. 6, bottom). A cross-correlation of the SIWEH of the vertical velocity with the sediment concentration (both at $z = 0.1$ m) indicated the sediment suspension to generally lag the vertical velocity events by some 2.5 s (maximum cross-correlation, $R = 0.32$). The proposed explanation for this is that turbulence (originating from the breakers at the surface) is recorded *en route* to the sea bed, with the sediment suspension caused by that turbulence occurring 2.5 s thereafter. Correlation of the sediment suspension record at 0.1 m with the vertical velocity events at $z = 0.4$ m yielded a higher correlation (maximum cross-correlation, $R = 0.43$), with the peak in suspension occurring 7.5 s after the peak in the vertical velocity events. The greater lag from the velocity events at a higher elevation may be indicative of the greater time delay for significant turbulence to penetrate the water column from the region nearer the surface, from which bore-generated

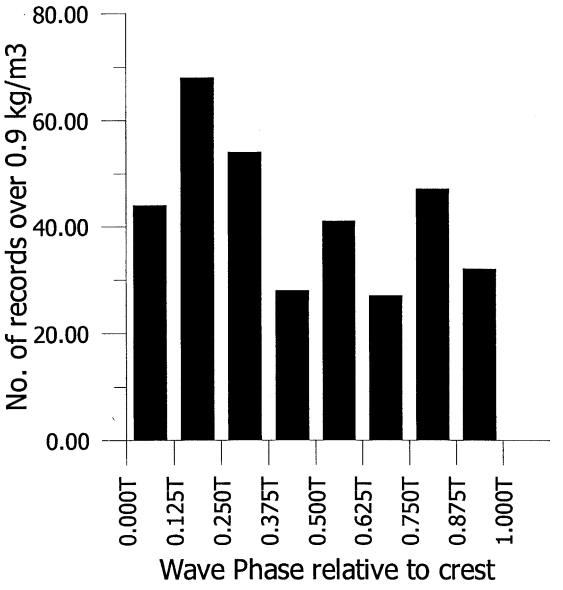

Fig. 7. Histogram illustrating the phase (relative to the wave peak) of the occurrence of sediment suspension concentrations that are significantly higher than the relatively constant background level (i.e. above 0.9 kg/m^3). LIP Test 2A, $X = 152$ m.

turbulence originates. Noting that the time delay between the vertical velocity event and sediment suspension is equivalent to around 1.5 wave periods, this finding also supports the concept of progressive stirring by successive waves.

5.1.2. Inner zone

As was conducted previously for the transition zone, the phase distribution of sediment suspension events throughout the wave cycle was investigated for the inner surf zone (LIP data, 53-min record). As can be seen from Fig. 7, the sediment suspension occurring in the form of events indicated a slightly higher occurrence soon after the wave peak (up to about one third of the wave period) but an otherwise random distribution of events throughout the wave cycle.

In the transition zone, the role of bores was highlighted through the identification of a high occurrence of bores occurring prior to suspension events, indicating surface-generated turbulence associated with these bores to be the cause of suspension. As bores occur almost all the time in the inner surf zone, an analysis of their effect on sediment suspension based on the frequency of their occurrence (as was possible for the transition zone) is not feasible. However, assuming that high-frequency velocity events are indicative of turbulence, such events are found to be almost as energetic (Fig. 8) as those observed in the highly dynamic transition zone despite the occurrence of smaller wave heights.

There is some indication that sediment suspension is related to the high-frequency vertical velocity events (Fig. 8), with the two major suspension events shown occurring within 2–7 s of such velocity activity. High-frequency vertical velocity activity was defined with the use of the SIWEH function (Fig. 8) as was done previously. Cross-correlation of this result with the sediment concentration for the 53-min time series indicates that sediment suspension at $z = 0.1$ m is correlated with the vertical velocity events at both 0.1 and 0.2 m elevation. In both cases the suspension lags the velocity event by about 3.5 s (maximum cross-correlation, $R = 0.32$ and 0.22 for the 0.1 and 0.2 m velocity elevations respectively) indicating that sediment suspension is induced by the high-frequency velocity events.

5.2. Time scale of surf zone sediment suspension and transport

While processes associated with incident breaking/broken waves are clearly indicated to be a cause of sediment suspension, this does not mean that sediment suspension and transport occurs on an incident time scale. The time scale of sediment suspension and transport flux was investigated by means of spectral analysis.

5.2.1. Transition zone

Velocity spectra derived from measurements in the transition zone for the LIP Tests 2A and 2B (Fig. 9a,b) manifest energy peaks in the infragravity range that are as high as or higher than the incident-scale peaks. Although the sediment spectra manifest limited periodic structure, the cospectra indicate distinct peaks (Figs. 9d–f). (It should be noted that in the case of the LIP data, the cospectra are derived with the assumption that the velocity time series at 0.1 m above the bed is

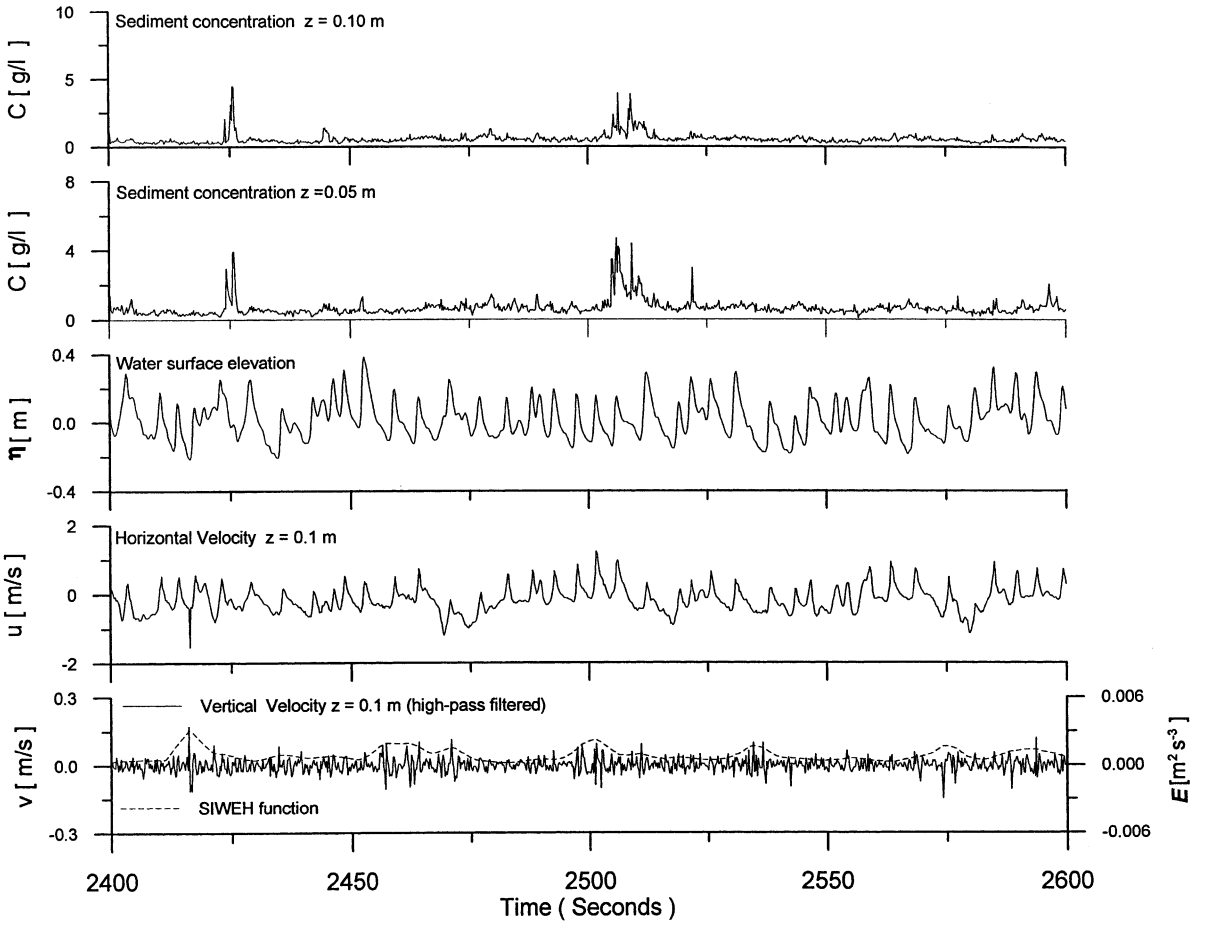

Fig. 8. Time series of sediment concentration and colocated velocities and surface elevations measured in the inner surf zone for LIP Test 2A ($X = 152$ m), and (bottom) the SIWEH function applied to the high-frequency (>1 Hz) vertical velocity record.

similar to that at 0.05 and 0.15 m. Comparison of velocities at 0.1 and 0.2 m indicates that this is the case; the velocities at these two elevations are virtually identical – measurements being linearly correlated with $R^2 = 0.97$). In the case of LIP Test 2A, flux was predominantly on an infragravity time scale; a significant oscillatory onshore flux is evident around 0.045 Hz (i.e. 22 s) and significant oscillatory offshore flux occurs at about 0.019 Hz (i.e. 53 s). Less-dominant onshore transport energy peaks occur at the incident wave frequency at the OBS elevations of 0.05 m, with those at 0.1 m and at 0.15 m being increasingly subdued (Fig. 9d). This decrease in sediment transport flux with increasing elevation from the bed is indicative of the increase in separation from the source of sand and sand transport at and near the bed.

In the case of Test 2B, infragravity-scale flux is also predominant; the suspension is correlated with the onshore phase of velocity such that a considerable onshore oscillatory flux results (Fig. 9e) at exactly the same frequency as for Test 2A (i.e. at 0.045 Hz). For this Test 2B (Fig. 9e) incident-scale flux is totally insignificant compared to that at infragravity frequencies, at all three OBS elevations. This may be because of the higher offshore wave height of Test 2B causing larger infragravity motions in the surf zone.

In the case of the Strand data, the peaks in the

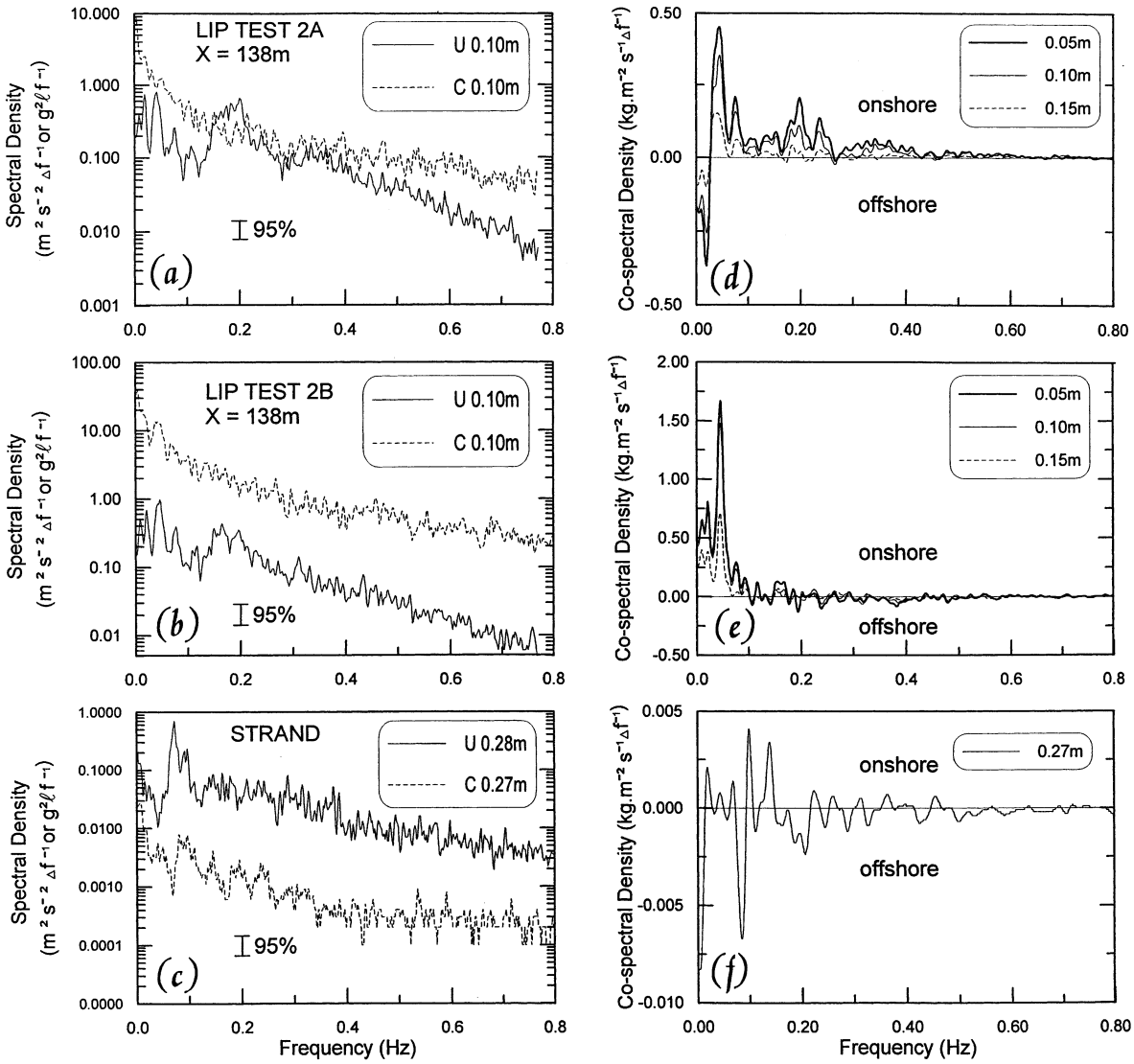

Fig. 9. Cross-shore velocity (u) and concentration (c) spectra and cospectra of these parameters, from measurements in the transition zone at Strand and LIP11D Tests 2A and 2B.

infragravity range of the velocity spectrum are slightly lower than those in the incident gravity wave range (Fig. 9c). This low-frequency energy (close to zero), evident in both the velocity and the sediment concentration spectra (Fig. 9c), is manifested in the cospectrum as well, which indicates a very low-frequency (around 0.005 Hz) oscillatory flux in the offshore direction (Fig. 9f). (It should be noted that in the calculation of the cospectrum, the velocity time series at 0.28 m above the bed is assumed to be essentially the same as that at 0.27 m). As seen in Fig. 9c, a minor peak in the sediment spectrum – of a similar magnitude to the infragravity flux – occurs at the incident wave frequency (0.08 Hz). This sediment suspension corresponds with an offshore flux at the incident wave frequency (Fig. 9f), indicating a link to the offshore phase of incident waves. This could be due to sediment suspended during onshore motion (or induced by wave-generated tur-

bulence penetrating to the bed) being transported during the offshore phase of orbital wave motion. The magnitude of spectral and flux estimates is lower than for the LIP cases; this is deemed to be due to the fact that the sediment sensor is situated further from the sea bed than for the LIP cases, and also possibly because of the more dissipative conditions during the Strand exercise.

5.2.2. *Inner surf zone*

In the inner surf zone during LIP11D Tests 2A and 2B, velocity energy at infragravity frequencies (Fig. 10a,b) is higher than that at incident wave frequency. While the sediment spectra of Tests 2A and 2B manifest little structure, offshore-directed infragravity-scale sediment transport flux is seen in the cospectra from Tests 2A and 2B at infragravity frequencies of 0.024 Hz (42 s) and 0.020 Hz (50 s). In the case of Test 2B, a notable onshore flux was also observed at 0.036 Hz (28 s). Incident velocity energy during both Tests 2A and 2B (Fig. 10a,b) is less than the infragravity component. The spectra of the sediment concentrations display no significant peaks at the incident wave frequency. This lack of significant suspension at the incident wave frequency is evident in the cospectra (Fig. 10c,d) where only minor peaks occur at the incident wave frequency of 0.2 Hz. The incident-scale flux is offshore and relatively insignificant, ranging from about 10% to about 35% of the energy at infragravity frequencies.

In sum, the spectral analysis indicates that sediment transport fluxes within the infragravity frequency band are dominant over fluxes related to incident wave frequencies in both the transition and inner surf zones. The exception to this finding is the occurrence of relatively small offshore flux (which is of similar magnitude to the infragravity flux) at the incident wave frequency occurring in the transition zone for the Strand case. Thus, while sediment suspension is largely caused by

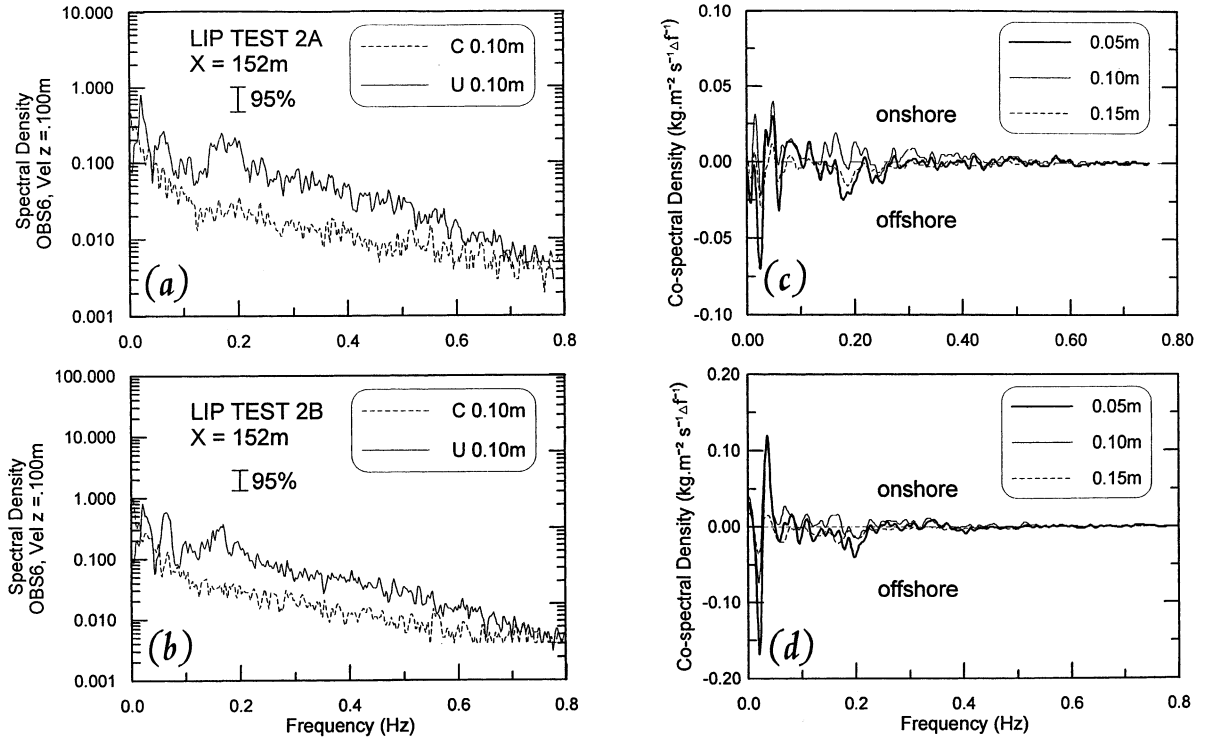

Fig. 10. Cross-shore velocity (u) and concentration (c) spectra and cospectra of these parameters, from measurements in the inner surf zone for LIP11D Tests 2A and 2B.

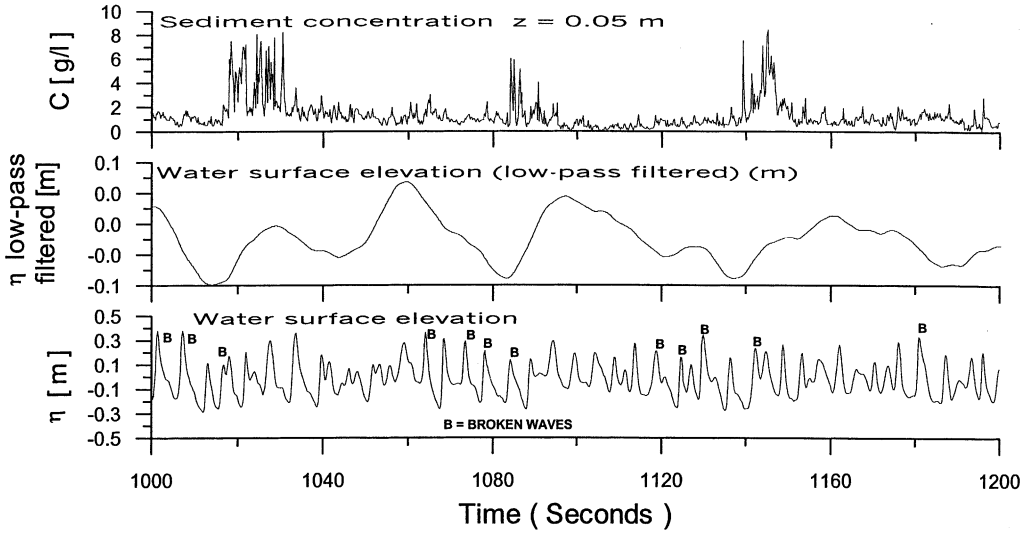

Fig. 11. Time series of near-bed sediment concentration (top), water surface elevation (bottom) and low-pass-filtered water surface elevation (< 0.05 Hz) (centre). Sediment suspension is evident soon after troughs in the latter time series (and after corresponding broken waves). Data are from LIP Tests 2A, $X = 138$ m.

incident breaking/broken waves in the surf zone, sediment transport flux is predominantly on an infragravity time scale. This may be explained by, for example, the occurrence of waves in the form of groups, and the successive stirring of sediment by successive waves in such groups.

Other mechanisms may also occur. For example, the occurrence of three suspension events just after low water-levels (obtained by means of filtering with a cut-off frequency of 0.05 Hz) can be discerned in Fig. 11. Correlating the filtered water-level with sediment concentration for the 53-min record indicated a maximum negative cross-correlation ($R = 0.27$) at a lag of about 7.5 s for Test 2A due to the correlation of the water-level trough with high sediment concentrations. As can be seen in Fig. 11, the periods of low mean water-level coincide with the passage of bores (as obtained from video recordings). Thus, the increased suspension just after low mean water-levels is deemed to be due to (1) the low water-level ensuring that wave breaking and/or bores occur (with their associated surface-generated turbulence) and/or (2) the source of the turbulence (i.e. the surface bore) being closer to the bed, implying a smaller distance for turbulence to travel. The correlation has a periodicity of about 27 s, corresponding with the peak frequency of infragravity wave energy. Thus a link between infragravity motions and sediment suspension by broken waves is discerned.

This type of relationship between low water-levels and suspension by bores does not always occur. A similar investigation with the Strand data, where long-wave activity was relatively subdued, indicated no relationship of sediment suspension to infragravity water-level fluctuations.

6. Discussion and conclusions

In this study insights were obtained into the functioning of the OBS as well as on the processes of sediment suspension by breaking and broken waves in the nearshore. Both physical and numerical methods exist to compensate for the OBS sensitivity to sand size (Black and Rosenberg, 1994), cohesive sediment in suspension (Green and Boon, 1993; Battisto et al., 1999), and organic material in suspension. The literature has indicated that bubbles do not have a major impact in field measurements (Black and Rosenberg, 1994). However, in the present small-scale laboratory measurements, where bubbles penetrate close to

the bed, they were found to cause an erroneous average increase of 32% in the concentration signal. This significant role of bubbles could possibly be the cause of inverted concentration profiles previously measured just shoreward of the initial breaking region with OBS, such as during Supertank (Barkaszi and Dally, 1992). The numerical filter employed was successful in removing 52% of the erroneous signal due to bubbles. Further work is proposed to refine this simple filter so as to be more effective.

Plots of time series indicated sediment suspension to be related to the occurrence of breaking/broken waves. On an incident scale, the influence of individual waves in the surf zone was indicated by a higher occurrence of event-driven sediment suspension occurring within half of a wave period after the passage of the wave crest. This effect was more prominent in the transition zone, where more energetic breaking of individual waves (particularly plunging waves) causes more significant suspension on an incident time scale.

Suspension events were also observed to occur after a series of breaking waves, as verified by a histogram analysis of the wave type (i.e. broken or unbroken) prior to suspension events in the transition zone. This result indicates a progressive increase in stirring that is induced by successive waves to be a cause of suspension. In addition, breaking/broken waves were observed to coincide with high-frequency (between 1 and 5 Hz) vertical velocity events, deemed to be a manifestation of turbulence (Hattori and Aono, 1985). Their occurrence in both the vertical and horizontal wave time series indicates that they are three-dimensional, i.e. possibly representing vertically descending eddies as proposed by Nadaoka et al. (1988).

Near-bed sediment suspension was found to lag vertical velocity events in the water column. The delay between these vertical velocity events higher in the water column ($z = 0.4$ m) and near-bed sediment suspension was greater than the delay between near-bed ($z = 0.1$ m) vertical velocity events and near-bed sediment suspension. This difference indicated the turbulence forcing to originate from the surface, in the transition zone. In the inner zone such a delay was not discernible, possibly because the measurements were closer (at $z = 0.1$ m and $z = 0.2$ m) and because vertical velocity events were less concentrated.

Sediment suspension and oscillatory transport flux were found to occur primarily at infragravity frequencies (rather than incident wave frequencies) in the surf zone, confirming previous results (Greenwood et al., 1991; Aagaard and Greenwood, 1994). While the Strand data was an exception to this finding, both the infragravity and incident time-scale fluxes were extremely small for this low-energy surf regime.

Previous studies maintained that this dominant infragravity flux in the surf zone is caused by infragravity-scale velocities both suspending and transporting sediment (e.g. Aagaard and Greenwood, 1994; Beach and Sternberg, 1988), However, the present study indicated a relationship of increased sediment suspension with low water-levels, which results in a predominance of wave breaking/broken waves; according to the findings of this study these waves are the cause of the suspension. Future work should be directed at confirming this initial finding and investigating other mechanisms of interaction between breaking/broken waves and infragravity-scale phenomena, such as wave groups.

Acknowledgements

The authors would like to acknowledge the cooperation of the EC MAST programme, in allowing the CSIR to contribute and gain access to data from the LIP11D flume exercise. In addition, the authors would like to acknowledge the contributions of Craig Fortuin, Dirk-Jan Walstra, Andre van der Westhuysen and Louise Watt to this study.

References

Aagaard, T., Greenwood, B., 1994. Sediment transport by wind waves, long waves and mean currents: an experiment on nearshore morphodynamics, Lake Huron, Canada. Coastal Dynamics '94, pp. 14–28.

Barkaszi, S.F., Jr., Dally, W.R., 1992. Fine-scale measurement

of sediment suspension by breaking waves at Supertank. Proc. 23rd Int. Conf. on Coastal Eng., pp. 1910–1923.

Battisto, G.M., Friedrichs, C.T., Miller, H.C., Resio, D.T., 1999. Response of OBS to mixed grain-size suspensions during Sandyduck '97. Coastal Sediments '99, pp. 297–312.

Beach, R.A., Sternberg, R.W., 1988. Suspended sediment transport in the surf zone: responses to cross-shore infragravity motion. Mar. Geol. 80, 61–79.

Black, K.P., Rosenberg, M.A., 1991. Hydrodynamics and Sediment Dynamics in Wave-Driven Environments. Volume 1: Field Equipment and Data. Victorian Institute of Marine Science, Technical Report No. 13.

Black, K.P., Rosenberg, M.A., 1994. Suspended sand measurements in a turbulent environment: field comparison of optical and pump sampling techniques. Coast. Eng. 24, 137–150.

Conner, C.S., De Visser, A.M., 1992. A laboratory investigation of particle size effects on an optical backscatterance sensor. Mar. Geol. 108, 151–159.

CSIR, 2000. Processes of Sediment Suspension and Transport in the Surf Zone and Shoaling Region from Optical Backscatter and Hydrodynamics Measurements. CSIR Report ENV-S-RR 2000-01.

Deigaard, R., Fredsoe, J., Broker-Hedegaard, I., 1986. Suspended sediment in the surf zone. J. Waterw. Port Coast. Ocean Eng. 112, 115–128.

Funke, E.R., Mansard, E.P.D., 1979. On the Synthesis of Realistic Sea States in a Laboratory Flume. Hydraulics Laboratory Report LTR-HY-66, NRC, Canada.

Green, M.O., Boon, J.D., 1993. The measurement of constituent concentrations in nonhomogeneous sediment suspensions using optical backscatter sensors. Mar. Geol. 110, 73–81.

Greenwood, B., Osborne, P.D., Bowen, A.J., 1991. Measurements of suspended sediment transport: Prototype shorefaces. Coastal Sediments '91, pp. 284–298.

Hanes, D.M., 1991. Suspension of sand due to wave groups. J. Geophys. Res. 96, 8911–8915.

Huntley, D.A., Hanes, D.M., 1987. Direct measurements of suspended sediment transport. Proc. Coastal Sediments '87, ASCE, pp. 723–737.

Hattori, M., Aono, T., 1985. Experimental study on turbulence structures under breaking waves. Coast. Eng. Jpn. 28, 97–116.

IMSL, 1991. User's Manual. FORTRAN Subroutines for Statistical Analysis. Version 2.0.

Kaiser, J.F., Reed, W.A., 1977. Data smoothing using low-pass digital filters. Rev. Sci. Instrum. 48, 1447–1457.

Kana, T., 1978. Surf zone measurements of suspended sediment. Proc. 16th Int. Conf. on Coastal Eng., ASCE, pp. 1725–1741.

Kineke, G.C., Sternberg, R.W., 1992. Measurements of high concentration suspended sediments using the optical backscatterance sensor. Mar. Geol. 108, 253–258.

Ludwig, K.A., Hanes, D.M., 1990. A laboratory evaluation of optical backscatterance suspended solids sensors exposed to sand-mud mixtures. Mar. Geol. 94, 173–179.

Mocke, G.P., Smith, G.G., 1992. Wave Breaker Turbulence as a Mechanism for Sediment Suspension. Proc. 23rd Int. Conf. on Coastal Eng., ASCE, pp. 2279–2292.

Nadaoka, K., Kondoh, T., 1982. Laboratory measurements of velocity field structure in the surf zone by LDV. Coast. Eng. Jpn. 25, 125–146.

Nadaoka, K, Ueno, S., Igarashi, T., 1988. Sediment suspension due to large scale eddies in the surf zone. Proc. 21st Int. Conf. on Coastal Eng., ASCE, pp. 1646–1660.

Nadaoka, K., Hino, M., Koyano, Y., 1989. Structure of the turbulent flow field under breaking waves in the surf zone. J. Fluid Mech. 204, 359–387.

Nielsen, P., 1984. Field measurements of time-averaged suspended sediment concentrations under waves. Coast. Eng. 8, 51–72.

NSRFC, 1975. NSRFC Wave Recording System (Type II Electronics): Product Description and Handbook, Report # COT 75-17, Centre for Ocean Technology, Nova Scotia Research Foundation Corporation.

Sanchez-Arcilla, A.S., Roelvink, J.A., O'Connor, B.A., Reniers, A., Jimenez, J.A., 1994. The Delta Flume '93 experiment. Coastal Dynamics '94, pp. 488–502.

Sato, S., Homma, K., Shibayama, T., 1990. Laboratory study on sand suspension due to breaking waves. Coast. Eng. Jpn. 33, 219–231.

Shibayama, T., Winyu, R., 1993. Vertical distribution of suspended sediment concentration in and outside the surf zone. Coast. Eng. Jpn. 36, 49–65.

Shibayama, T., Higuchi, A., Horikawa, K., 1986. Sediment transport due to breaking waves. Proc. 20th Coastal Eng. Conf., ASCE, pp. 1509–1522.

Smith, G.G., Mocke, G.P., Engelbrecht, L., 1995. Sediment transport fluxes as determined from wave breaker induced suspended sediment and flow fields. Proc. Coastal Dynamics Conf. '95, pp. 783–794.

Stive, M.J.F., 1980. Velocity and pressure field of spilling breakers. Proc. 17th Coastal Eng. Conf., pp. 547–566.

Villard, P.V., Osborne, P.D., Vincent, C.E., 1999. Influence of wave groups on sand re-suspension in a large scale wave flume. Coastal Sediments '99, pp. 367–376.

Yu, Y., Sternberg, R.W., Beach, R.A., 1993. Kinematics of breaking waves and associated suspended sediment in the nearshore zone. Cont. Shelf Res. 13, 1219–1242.